# Geochemical and Petrological Characterization of the Early Eocene Carbonaceous Shales: Implications for Oil and Gas Exploration in the Barmer Basin, Northwest India

Alok Kumar, Mohammed Hail Hakimi,* Alok K. Singh, Wan Hasiah Abdullah,
Nor Syazwani Zainal Abidin, Afikah Rahim, Khairul Azlan Mustapha, and Nura Abdulmumini Yelwa

ACCESS | Metrics & More | Article Recommendations

**ABSTRACT:** Carbonaceous shales of the Early Eocene Dharvi/Dunger Formation in the onshore Barmer Basin, northwest India were studied for the first time by integrating geochemical and organic petrological analyses. The carbonaceous shales of the Early Eocene Dharvi/Dunger Formation are characterized by a higher organic carbon content (TOC) of >10 wt % and consist mainly of a mixture of organic matter of types II and III kerogen, with exhibited hydrogen index values ranging between 202 and 292 mg HC/g TOC. The dominance of such kerogen is confirmed by the high amounts of huminite and fluorescent liptinite macerals. Consequently, the carbonaceous shales of the Early Eocene Dharvi/Dunger Formation are promising source rocks for both oil and gas generation potential, with oils of high wax contents, according to pyrolysis−gas chromatography results. The chemical and optical maturity results such as low values huminite/vitrinite reflectance, production index, and $T_{max}$ show that most of the examined carbonaceous shale rocks from the outcrop section of the Kapurdi mine have entered the low maturity stage of oil generation, exhibiting a range of immature to the very early-mature. Therefore, as highlighted in this study, the substantial abundance in hydrocarbon generation potential from these carbonaceous shales in the Dharvi/Dunger Formation may represent future conventional petroleum exploration in the southern part of the Barmer Basin, where the Dharvi/Dunger Formation has reached deeper burial depths.
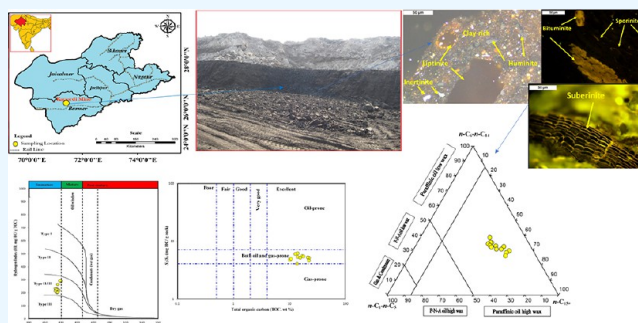
## 1. INTRODUCTION

The Barmer Basin is a shallow marine failed rift[1] and is located in the Desert of Thar in the west part of the Rajasthan region, NW India (Figure 1). This basin together with other interior rift basins in India is associated with the rifting mechanisms associated with the split of Gondwana land.[2] Zhu et al.[2] suggested that the India plate was rapidly separated from the Africa plate during the Jurassic Period, and subsequently the continental drift of Madagascar and the Seychelles was affiliated due to the colliding between Indian and Asian plates. However, Farrimond et al.[3] reported that the Barmer Basin was an active rift basin that formed during the Late Jurassic to Cretaceous Period, creating an asymmetrical half-graben, bounded on the eastern side by a major NNW-trending border fault systems, and categorized as downwarped, horst, and slanted blocks (shown in Figure 2).

The Barmer Basin includes sedimentary successions, ranging in age between Mesozoic and Cenozoic, with several significant unconformities (Figure 3). The clay-rich rocks of the Mesozoic and Cenozoic successions are an important organic-rich clay facies for exploration, development and production targets in the Barmer Basin.[1] Organic-rich shales of the Cretaceous to Paleocene formations (Figure 3) were geochemically investigated to estimate their potential as source rock for hydrocarbon generation potential by applying conventional geochemical results, including the content of total organic carbon (TOC) and conditioned programmed pyrolysis.[1]

Dolson et al.[1] concluded that the organic-rich shale sequences of the Late Paleocene Barmer Hill Formation are considered to be the main source rocks for hydrocarbon exploration in the Barmer Basin. The Barmer Hill organic-rich shales were deposited in lacustrine settings and consist mainly of types I and II kerogens along with mixed type II/III kerogens; consequently, they are mainly oil- and gas-prone source
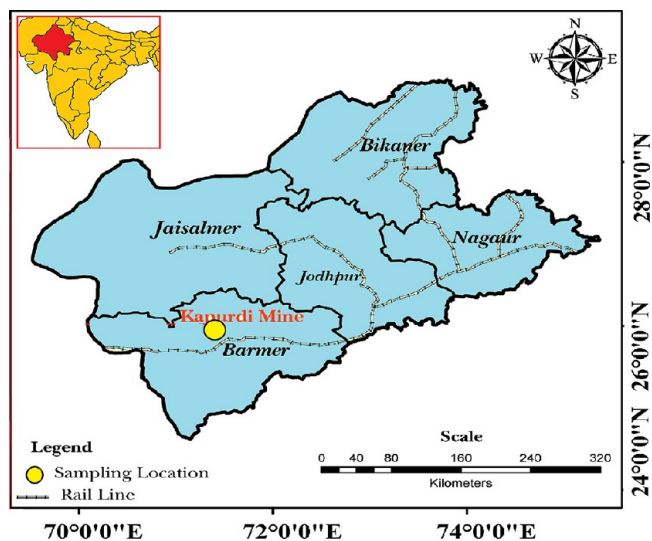
**Figure 1.** Location map of the main basins in Rajasthan, northwestern India, showing the Kapurdi mine location in the northern Barmer Basin.

rocks.[1] This finding is confirmed by the good geochemical correlations between the reservoir oils and the mature Barmer

Hill source rock in the basin.[3] Farrimond et al.[3] examined the biomarker fingerprints of reservoir oils in the basin and extensively documented that there are three oil families in the Barmer Basin, and the Barmer Hill source rock is the furthermost oil-source rock and directly interrelated with the main petroleum-producing regions recognized to date, which is acting as a conventional petroleum resource.

While Dolson et al.[1] and Farrimond et al.[3] reported that the organic-rich shales of the Late Paleocene Barmer Hill Formation are an important source rock potential for conventional exploration and production targets in the southern part of the Barmer Basin, little is known about the organic-rich shale found in the Early Eocene successions, especially those from the Dharvi/Dunger Formation (Figure 3), which is the primary objective of this study. The Dharvi/Dungar Formation has mainly lacustrine black shale intervals with interbedded swamp lignites (Figure 3), which was deposited in lacustrine environmental setting.[1] However, the characteristics of organic matter and the petroleum potential of these lacustrine black shales are limited, and large-scale commercial development and production for conventional and unconventional petroleum resources have not yet been realized. In this case, multigeochemical methods and microscopic investigations are combined to characterize the organic matter and determine petroleum
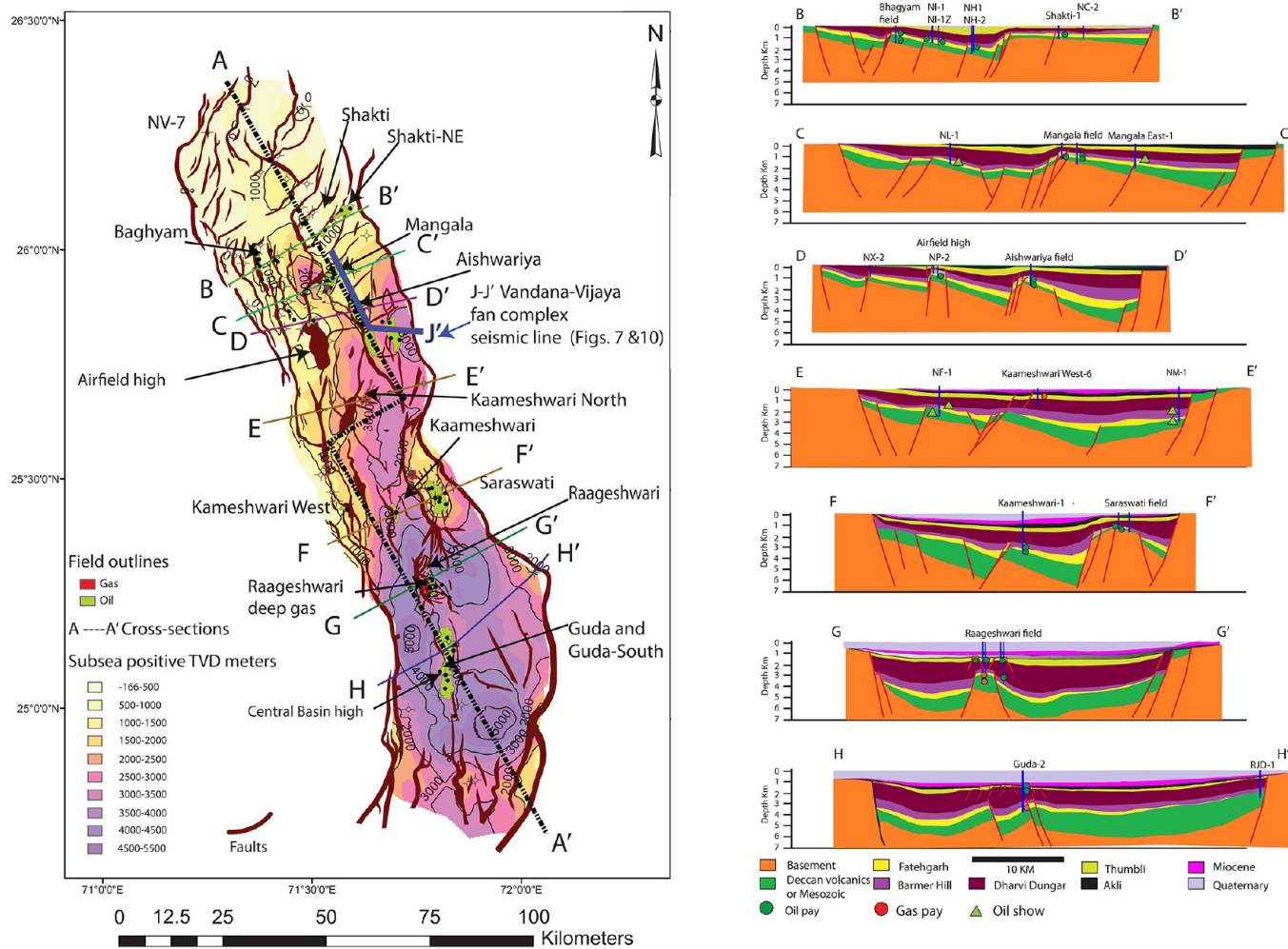


**Figure 2.** Left: Fatehgarh structure map showing the locations of major fields, wells, and seismic section. Right: representative geo-seismic west−east structural cross section drawn from regional 2D seismic lines down the basin, illustrating the major structural features of the Barmer Basin (compiled from Dolson et al.[1]).
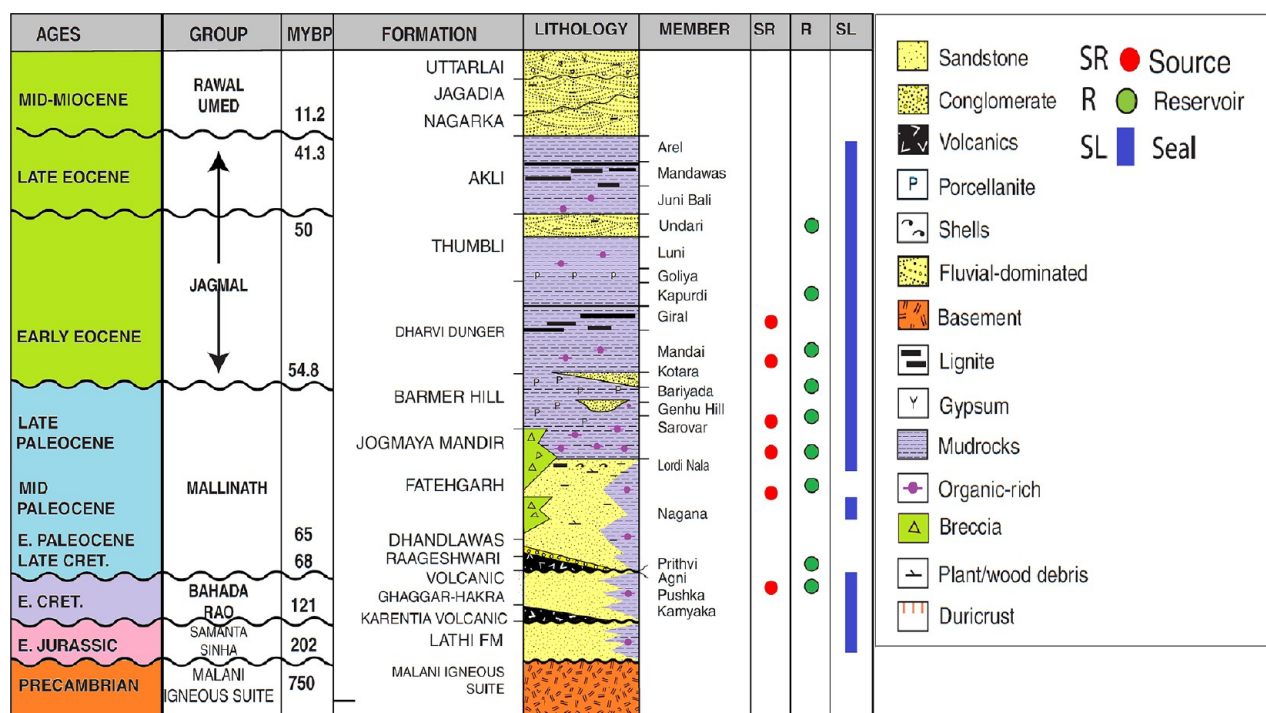
**Figure 3.** Generalized stratigraphic column in the Barmer Basin, including igneous rocks and sedimentary sequence (compiled from Dolson et al.[1]).



**Figure 4.** Photographs of the outcrop section in the Kapurdi mine.

generation potential of the black shale horizons within the early Eocene Dharvi/Dunger Formation.

The objectives of this study were to (1) determine the organic matter content, (2) identify the kerogen classification, and (3) assess the petroleum generation potential by employing multiple geochemical techniques tied with microscopic investigation. Moreover, this study discusses the utility of the results obtained from the current research to outline the attributes of the conventional petroleum exploration along the basin.

## 2. MATERIALS AND EXPERIMENTAL METHODS

In this study, 13 organic-rich rock samples (i.e., carbonaceous shale) were collected from the early Eocene Dharvi/Dunger Formation that outcrops at the Kapurdi mine area (Figure 4).

The carbonaceous shale samples were subjected to multi-geochemical methods, including Rock-Eval pyrolysis, total organic carbon (TOC) content, and pyrolysis−gas chromatography (Py-GC) analyses along with microscopic examinations of the maceral types and reflectance measurements of huminite/vitrinite (%$VR_o$).

Polished sample blocks were investigated under a microscope for the identification of organic facies.[4] The polished blocks underwent examination using oil immersion under both reflected white and ultraviolet (UV) light using a LEICA DM 2700P optical microscope coupled with a fluorescence illuminator photometry microscope.

In this case, entire whole rock samples were broken into small pieces (about 2−3 mm, pea sized) and implanted into molds
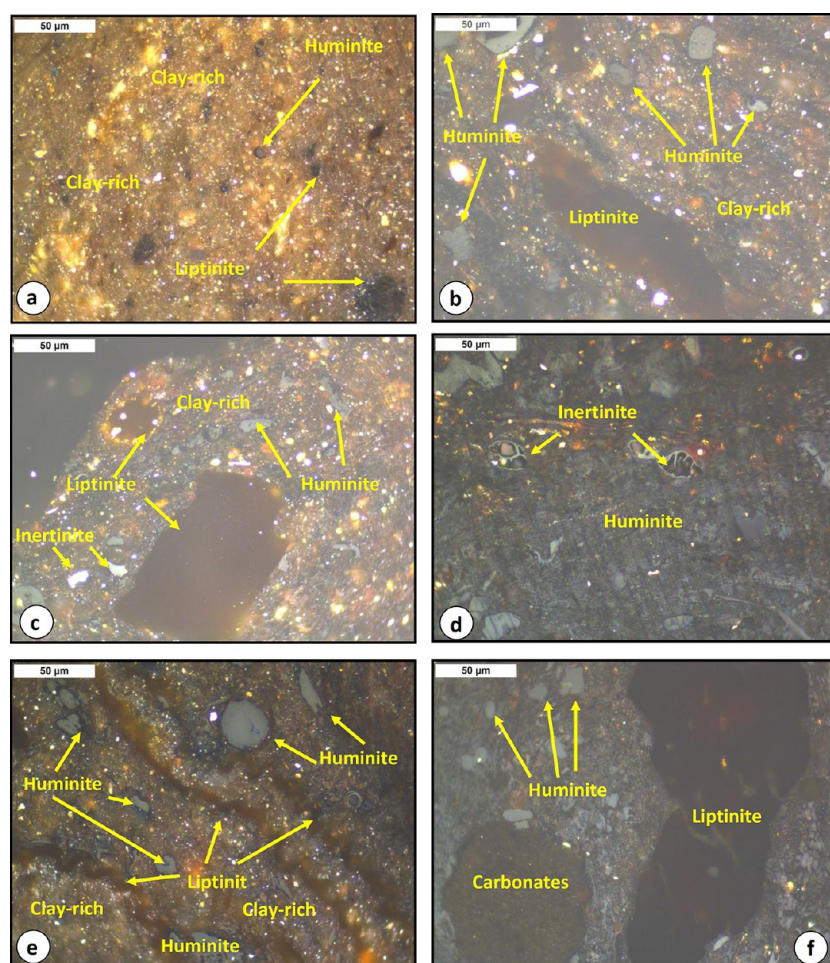
**Figure 5.** Photomicrographs of maceral types from the analyzed carbonaceous shale rocks, under normal light, field width = 0.2 mm, including (a−c) clay minerals associated with structured and unstructured huminite, liptinite, and inertinite macerals, (d) mainly structured huminite, liptinite, and inertinite macerals, (e) mainly structured liptinite associated with huminite, and (f) carbonate minerals associated with unstructured liptinite and huminite macerals.

employing a SeriFix resin with a cold-mount hardener combination. After hardening, the blocks were ground to expose the sample surfaces using silicon carbide sheets with varying grit sizes; they were singly polished using alumina powder and oxide-polishing suspension solution.

The reflectance of huminite/vitrinite ($VR_o$) measurements was also performed on the polished blocks using reflected white light. $\%VR_o$ was measured after calibration using a reflectance standard value of 0.420% (spinel), 0.902% (yttrium-aluminum-garnet), and 1.71% (gadolinium-gallium-garner) under oil immersion, and the mean of reflectance values were calculated for 30 points for each sample.

In addition, quantitative and qualitative analyses of maceral types, including huminite, liptinite, and inertinite, were carried out following Hower and Wagner,[5] Pickel et al.,[6] and ICCP.[7] In this case, reflected UV lights were used to discriminate maceral types for each sample.

For the geochemical evaluation, the organic carbon (TOC wt %) and total sulfur (TS wt %) contents were measured from pulverized samples (<200 mesh) using a Carbon/Sulfur Analyzer (LECO CS244).

Bulk pyrolysis was carried out on powdered sample's using a programmed pyrolysis (Rock-Eval 6) machine in accordance with the techniques specified by Lafargue et al.[8] From these analyses, the maximum temperature for $S_2$ production ($T_{max}$),

the number of free hydrocarbons prior to pyrolysis ($S_1$), post-pyrolysis residual hydrocarbons ($S_2$), and the amount of $CO_2$ generated by kerogen pyrolysis ($S_3$, mg/g) were obtained. In addition, hydrocarbon potential (PY = $S_1$ + $S_2$), production index (PI = $S_1/S_1$ + $S_2$), hydrogen index (HI = $S_2 \times 100/TOC$), and oxygen index (OI = $S_3 \times 100/TOC$) were also determined utilizing the TOC and bulk pyrolysis data.[9]

Subsequently, bitumen was extracted from the analyzed carbonaceous shale using standard techniques. Briefly, 20−25 g of each crushed sample was dispersed volumetrically in solution of 93% dichloromethane and 7% methanol utilizing Soxhlet apparatus for 72 h.

The extracted samples were then reserved for further geochemical analysis such as Py-GC outlined by Larter.[10] In doing so, $S_2$ compositions and their kerogen characteristics were identified. A pyrolysis system (Frontier Laboratories, Koriyama, Japan) was used to analyze about 1−2 mg of extracted material via Py-GC. The pyrolysate was heated in the Py-GC furnace at a rate of 4 °C/min from 40 to 300 °C, and the pyrolysate went through the GC column at temperatures ranging from 300 to 600 °C. In addition to a methane peak, the chromatography results revealed a set of *n*-alkane and *n*-alkene double peaks as well as some aromatic peaks between them.
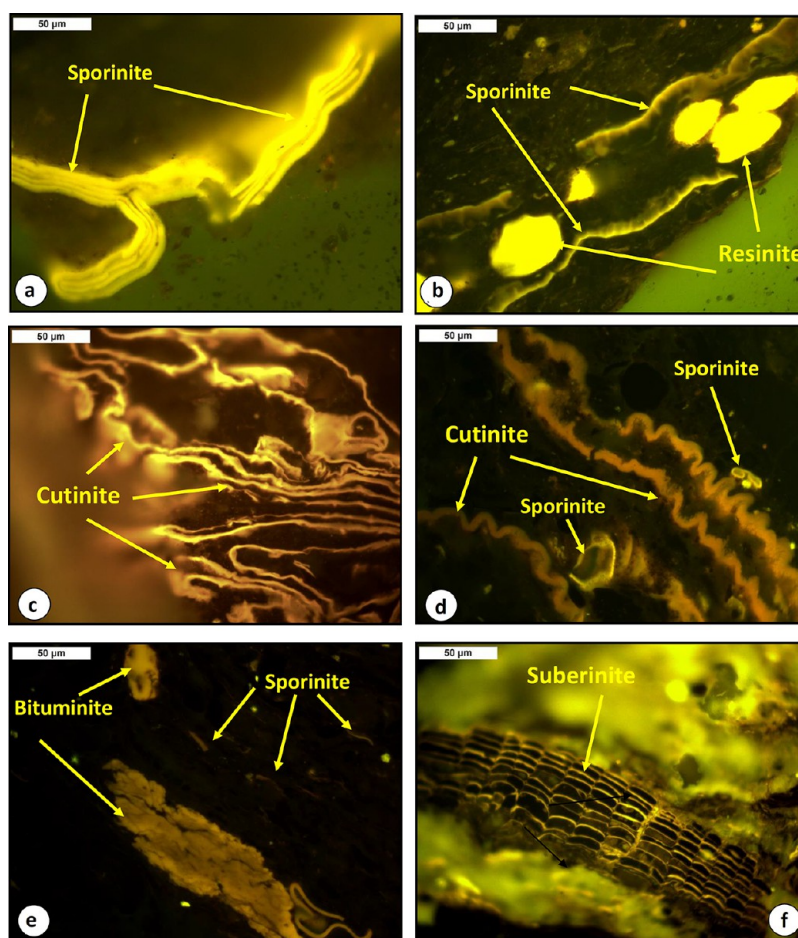
**Figure 6.** Photomicrographs of liptinite macerals from the analyzed carbonaceous shale rocks, under UV light, field width = 0.2 mm, including structured and unstructured fluorescence of (a) sporinite, (b) sporinite and resinite, (c, d) cutinite, (e) bituminite, and (f) suberinite.

**Table 1. Petrographic Analysis of the Analyzed Kapurdi Carbonaceous Shale Samples from the Kapurdi Mine in the Barmer Basin, NW India Covers of Huminite/Vitrinite Reflectance (VR$_o$ %) and Maceral Counting Percentage along with Basis of Mineral Matter (vol %) and Mineral-Matter-Free (vol %)**

| sample ID | maceral composition (%) | | | mineral matter (%) | maceral composition (free minerals %) | | | huminite/vitrinite reflectance (VR$_o$ %) | | | |
|---|---|---|---|---|---|---|---|---|---|---|---|
| | huminite | liptinite | inertinite | | huminite | liptinite | inertinite | mean | minimum | maximum | SD |
| KD-T2 | 10.00 | 4.15 | 0.00 | 85.85 | 70.67 | 29.33 | 0.00 | 0.37 | 0.27 | 0.46 | 0.056 |
| KD-T3 | 22.53 | 3.16 | 0.14 | 74.17 | 87.22 | 12.23 | 0.54 | 0.39 | 0.26 | 0.51 | 0.054 |
| KD-T4 | 9.89 | 2.40 | 0.28 | 87.43 | 78.68 | 19.09 | 2.23 | 0.41 | 0.29 | 0.51 | 0.073 |
| KD-T5 | 17.74 | 3.33 | 0.37 | 78.56 | 82.74 | 15.53 | 1.73 | 0.52 | 0.34 | 0.67 | 0.085 |
| KD-T6 | 7.03 | 2.72 | 0.00 | 90.25 | 72.10 | 27.90 | 0.00 | 0.47 | 0.35 | 0.55 | 0.067 |
| KD-T8 | 26.01 | 5.90 | 0.55 | 67.54 | 80.13 | 18.18 | 1.69 | 0.28 | 0.21 | 0.37 | 0.049 |
| KD-T-9 | 11.19 | 8.48 | 0.29 | 80.04 | 56.06 | 42.48 | 1.45 | 0.28 | 0.20 | 0.36 | 0.050 |
| KD-M1 | 13.15 | 6.97 | 0.32 | 79.56 | 64.33 | 34.10 | 1.57 | 0.33 | 0.24 | 0.44 | 0.059 |
| KD-M2 | 4.96 | 3.72 | 0.21 | 91.11 | 55.79 | 41.84 | 2.36 | 0.36 | 0.33 | 0.40 | 0.026 |
| KD-M3 | 5.87 | 3.39 | 0.45 | 90.29 | 60.45 | 34.91 | 4.63 | 0.38 | 0.26 | 0.46 | 0.071 |
| KD-B2 | 12.35 | 15.23 | 0.82 | 71.60 | 43.49 | 53.63 | 2.89 | 0.29 | 0.21 | 0.35 | 0.046 |
| KD-B3 | 14.19 | 14.19 | 1.40 | 70.22 | 47.65 | 47.65 | 4.70 | 0.30 | 0.26 | 0.33 | 0.029 |
| KD-B4 | 31.15 | 19.04 | 5.58 | 44.23 | 55.85 | 34.14 | 10.01 | 0.30 | 0.22 | 0.39 | 0.061 |

## 3. RESULTS AND DISCUSSION

### 3.1. Organofacies Characteristic under Microscopic Examination.
Microscopic examination was carried out to identify maceral types of the analyzed Kapurdi carbonaceous shales. The results exhibit that these samples dominantly comprise mineral matter and host different maceral types, as determined based on mineral matter and mineral matter-free and depicted in the microphotographs of Figures 5 and 6.

The analyzed carbonaceous shale samples are dominated by mineral matter between 44.23% and 91.11% (Table 1). The mineral matter fraction is dominated by clay minerals as shown in the microphotographs in Figure 5. On a mineral matter-free basis, the carbonaceous shale samples have a high abundance of
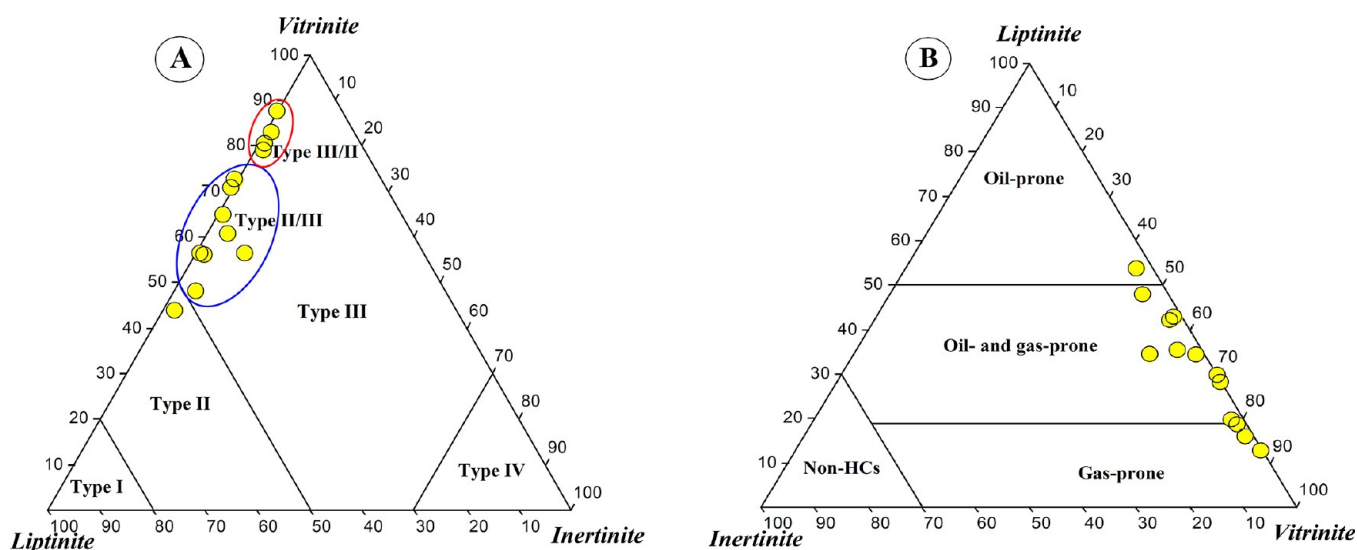
**Figure 7.** Ternary diagrams on (A) the kerogen characteristics based on the relative percentage of maceral types, showing that the analyzed carbonaceous shale samples are dominated by type II/III and III/II kerogen, and (B) the relative percentage of maceral types, showing that the analyzed carbonaceous shale samples can generate mainly high waxy paraffinic oil, with limited gas.

the huminite maceral group, ranging from 43.49% to 87.22% (Table 1). As per the analysis reported from optical observations under reflected white light, the huminite maceral is primarily brittle with an angular surface and varying shapes (Figure 5b−f). In contrast with huminite maceral, liptinite macerals dominated all of the samples, with a range of 12.23%−53.63% (Table 1). These macerals appeared brown−dark brown under reflected white light (Figure 5). The fluorescence intensities vary from orange to yellow when exposed to UV light (Figure 6). UV-light excitation was mainly used to distinguish between liptinite assemblages and shows that most of the samples have medium to low structured and unstructured hydrogen-rich liptinite macerals, as shown in Figure 6. In this case, most of the examined samples showed structured macerals, including suberinite, cutinite, and sporinite (Figure 6). Sporinite occurs as macro- or microsporinite in a ring-agglomerated form (Figure 6a,b,d,e). Cutinite always takes a strand-like form, which is commonly associated with sporinite,[16] having yellow to orange-yellow fluorescence colors (Figure 6c and d). Suberinite is also represented and characterized by cell-wall tissue and has fluorescence intensities ranging from brownish-yellow to yellow (Figure 6f).

Indigenous structureless bituminite and resinite were also observed in a few cases (Figure 6e). Resinite mainly takes the form of isolated globular bodies with various shapes, and it is characterized by bright yellow fluorescence (Figure 6b). These resinite macerals are mostly structurally aligned, and they enclose vitrinite in separate globular bodies, showing a possibility of microlamination occurrence.[11] A bituminite with an irregular surface and orange to brownish yellow fluorescence colors was also found in the studied samples (Figure 6e). In addition, a small portion of inertinite maceral was also common in the analyzed samples (0.00−10.01%; Table 1). This maceral is represented by angular surfaces, varying shapes, and high reflectance mode under reflected white light (Figure 5c,d).

The huminite, liptinite, and inertinite macerals (Table 1) were utilized to characterize the organofacies and their kerogen types in these carbonaceous shales. The observations drew inspiration from the ternary diagram initially presented in the work of Abdullah et al.[12] Accordingly, from the analysis of samples, it was

observed that they contained a mixture of organic matter, exhibiting a gradient from type II/III to type III/II kerogen (Figure 7A). Most of the investigated shale samples have high contributions of huminite, and liptinite macerals are likely type II/III kerogen (Figure 7A). Further, samples with more than 70% huminite macerals were likely to be type III/II kerogen (Figure 7A). The significant fraction of huminite and fluorescent liptinites under UV light (Figure 6) confirms both oil and gas-prone, with strong oil generative potential (Figure 7A). However, most of the hydrogen-rich liptinite macerals (i.e., sporinite, resinite, cutinite, and suberinite) in the analyzed samples (Figure 6) can generate paraffinic oil with a high waxy characteristic as reported by previously published works of Taylor et al.[4] and Petersen et al.[11] Other samples contain hydrogen-poor huminite maceral that derived from land plants and can generate mainly gas (Figure 7B).

Additionally, the reflectance of the huminite/vitrinite maceral (VR$_o$) in the studied samples was measured and the maximum, minimum, and mean values are shown in Table 1. Such values are the most reliable indicator to highlight the maturity and highlight the critical information such as the degree of maturation of organic material and the ability to generate petroleum.[13] The studied samples have mean values of the huminite/vitrinite reflectance (VR$_o$) between 0.28% and 0.52% (Table 1), indicating immature to the very early mature oil-window. Most of the samples have VR$_o$ values less than 0.50%, which suggests immature organic matter. The highest VR$_o$ value of 0.52% (Table 1) suggests that this sample reached a very early mature of oil generation window.

**3.2. Organic Carbon and Sulfur Contents.** A sufficient amount of organic carbon content is a prerequisite for the ability to generate hydrocarbons during maturation.[13,14] The organic carbon content is termed as TOC and reported as a function of wt %, and these values most commonly infer the presence of OM richness.[14,15] The majority of geochemists feel that sediments rich in organic matter with a TOC level of more than 1% suggest a favorable source of petroleum potential.[15]

In this study, measured TOC values of all Kapurdi carbonaceous shale samples exhibit a TOC range of 10.24%− 22.42% (Table 2). Majority of the measurements indicate TOC

**Table 2. Geochemical Results of TOC, TS Contents, Bulk Rock-Eval Pyrolysis and Pyrolysis-Gas Chromatography (Py-GC) of the Analyzed the Analyzed Kapurdi Carbonaceous Shale Samples from Kapurdi Mine in the Barmer Basin, NW India[a]**

| samples ID | TOC wt % | TS wt % | bulk Rock-Eval pyrolysis measured $S_1$ (mg/g) | $S_2$ (mg/g) | $S_3$ (mg/g) | $T_{max}$ (°C) | HI (mg/g) | OI (mg/g) | calculated PY (mg/g) | PI (mg/g) | $S_2/S_3$ (mg/g) | pyrolysis-gas chromatography (Py-GC) $n$-$C_9$ (%) | xylene (%) | 2,3-dimethylthiophene (%) | xy/$C_8$ ratio | $C_8$/xy ratio | $C_1$-$C_5$ (%) | $C_6$-$C_{14}$ (%) | +$C_{15}$ (%) |
|---|---|---|---|---|---|---|---|---|---|---|---|---|---|---|---|---|---|---|---|
| KD-T2 | 16.94 | 0.51 | 0.44 | 39.44 | 7.15 | 423 | 233 | 42 | 39.88 | 0.01 | 5.52 | 42.27 | 37.80 | 19.93 | 0.67 | 1.50 | 15.82 | 31.99 | 52.19 |
| KD-T3 | 21.66 | 0.54 | 0.53 | 47.76 | 9.29 | 427 | 220 | 43 | 48.29 | 0.01 | 5.14 | 42.26 | 38.71 | 19.03 | 0.76 | 1.31 | 21.16 | 30.39 | 48.45 |
| KD-T4 | 14.01 | 0.38 | 0.38 | 32.08 | 6.00 | 425 | 229 | 43 | 32.46 | 0.01 | 5.35 | 43.29 | 36.79 | 19.92 | 0.62 | 1.62 | 15.94 | 28.19 | 55.87 |
| KD-T5 | 22.42 | 0.50 | 0.51 | 49.12 | 9.51 | 425 | 219 | 42 | 49.63 | 0.01 | 5.17 | 40.07 | 40.07 | 19.87 | 0.78 | 1.28 | 23.23 | 32.78 | 43.99 |
| KD-T6 | 17.82 | 0.41 | 0.40 | 40.49 | 7.42 | 425 | 227 | 42 | 40.89 | 0.01 | 5.46 | 45.00 | 31.67 | 23.33 | 0.95 | 1.05 | 14.28 | 28.96 | 56.76 |
| KD-T8 | 22.24 | 0.40 | 0.52 | 45.97 | 9.91 | 425 | 207 | 45 | 46.49 | 0.01 | 4.64 | 37.88 | 32.83 | 29.29 | 0.68 | 1.46 | 22.94 | 31.81 | 45.25 |
| KD-T-9 | 21.31 | 0.45 | 0.53 | 48.19 | 9.19 | 424 | 226 | 43 | 48.72 | 0.01 | 5.24 | 44.67 | 36.31 | 19.02 | 0.62 | 1.60 | 20.19 | 32.50 | 47.31 |
| KD-M1 | 13.68 | 1.43 | 0.54 | 27.65 | 6.77 | 425 | 202 | 49 | 28.19 | 0.02 | 4.08 | 38.50 | 34.07 | 27.43 | 0.63 | 1.60 | 18.10 | 30.40 | 51.50 |
| KD-M2 | 10.24 | 0.51 | 0.28 | 20.90 | 4.38 | 426 | 204 | 43 | 21.18 | 0.01 | 4.77 | 40.54 | 38.08 | 21.38 | 0.61 | 1.65 | 21.59 | 34.67 | 43.74 |
| KD-M3 | 10.70 | 0.67 | 0.36 | 22.86 | 4.59 | 423 | 214 | 43 | 23.22 | 0.02 | 4.98 | 40.86 | 37.63 | 21.51 | 1.17 | 0.86 | 18.14 | 25.65 | 56.21 |
| KD-B2 | 15.59 | 0.35 | 0.60 | 41.19 | 7.97 | 426 | 264 | 51 | 41.79 | 0.01 | 5.17 | 48.32 | 32.54 | 19.13 | 0.59 | 1.69 | 21.50 | 34.30 | 42.30 |
| KD-B3 | 14.07 | 0.58 | 0.68 | 40.68 | 6.59 | 430 | 289 | 47 | 41.36 | 0.02 | 6.17 | 50.83 | 35.33 | 13.84 | 0.50 | 1.99 | 20.61 | 37.34 | 40.05 |
| KD-B4 | 12.75 | 0.59 | 0.62 | 37.18 | 6.18 | 429 | 292 | 48 | 37.80 | 0.02 | 6.02 | 51.98 | 30.75 | 17.26 | 0.58 | 1.72 | 23.77 | 33.52 | 41.71 |

[a]TOC: Total organic carbon, wt %, TS: total sulfur, wt %, $S_1$: volatile hydrocarbon (HC) content, mg HC/g rock, $S_2$: remaining HC generative potential, mg HC/g rock, $S_3$: carbon dioxide content, mg CO$_2$/g rock, $T_{max}$: temperature at maximum of the $S_2$ peak, HI: hydrogen index = $S_2 \times 100$/TOC, mg HC/g TOC; OI: oxygen index = $S_3 \times 100$/TOC, mg CO$_2$/g TOC, PY: potential yield = $S_1 + S_2$ (mg/g), PI: production index = $S_1/(S_1 + S_2)$; 2,3 Dimeth. (%) − percent concentration of 2,3 dimethylthiopene in relation to O-xylene and $n$-C9; O-xylene (%) − percent concentration of O-xylene in relation to 2,3 dimethylthiopene and $n$-C9; $n$-C9 (%) − percent concentration of $n$-C9 in relation to 2,3 dimethylthiopene and O-xylene.
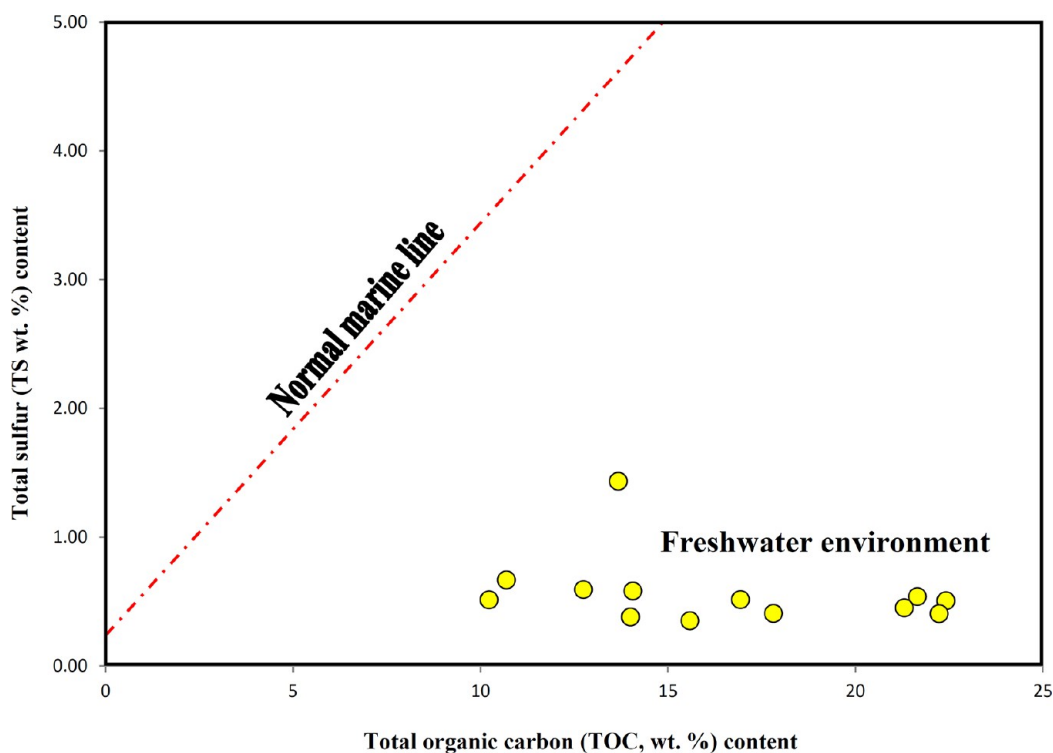
**Figure 8.** Cross plot of the sulfur and TOC contents (wt %), suggesting a lacustrine environment during deposition of the analyzed carbonaceous shales.
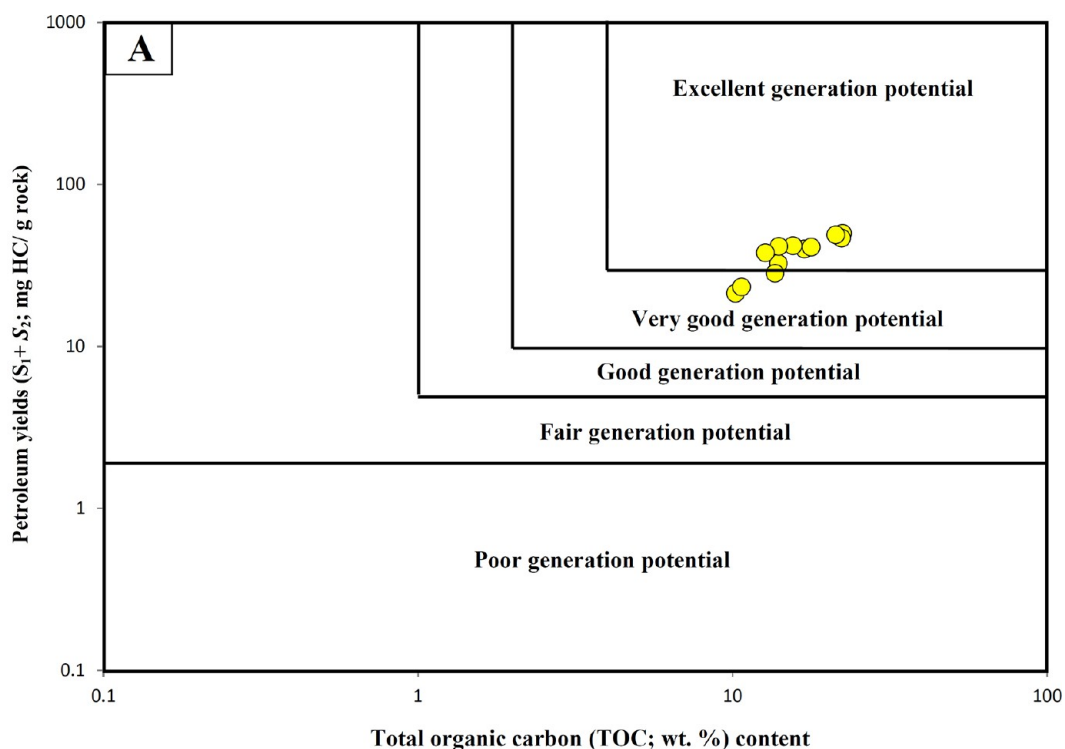


**Figure 9.** Geochemical correlations between TOC content and Rock-Eval pyrolysis ($S_1$ and $S_2$) parameters, implying that the analyzed carbonaceous shales from Kapurdi mines are considered to have very good to excellent generation potential.

< 20 wt % (10.24%−17.82%), while the other four samples have the highest values of TOC content between 21.31% and 22.42% (Table 2). Overall, the TOC contents of the studied shale samples indicate organic matters richness capable of generating hydrocarbons.[13−15]

The total sulfur (S) content in the studied samples was also measured and found to be in the low amounts in the range of 0.35 and 1.43 wt % (Table 2). The total S content is usually employed to investigate the depositional environments of marine versus non-marine.[16] A high S content of more than 1
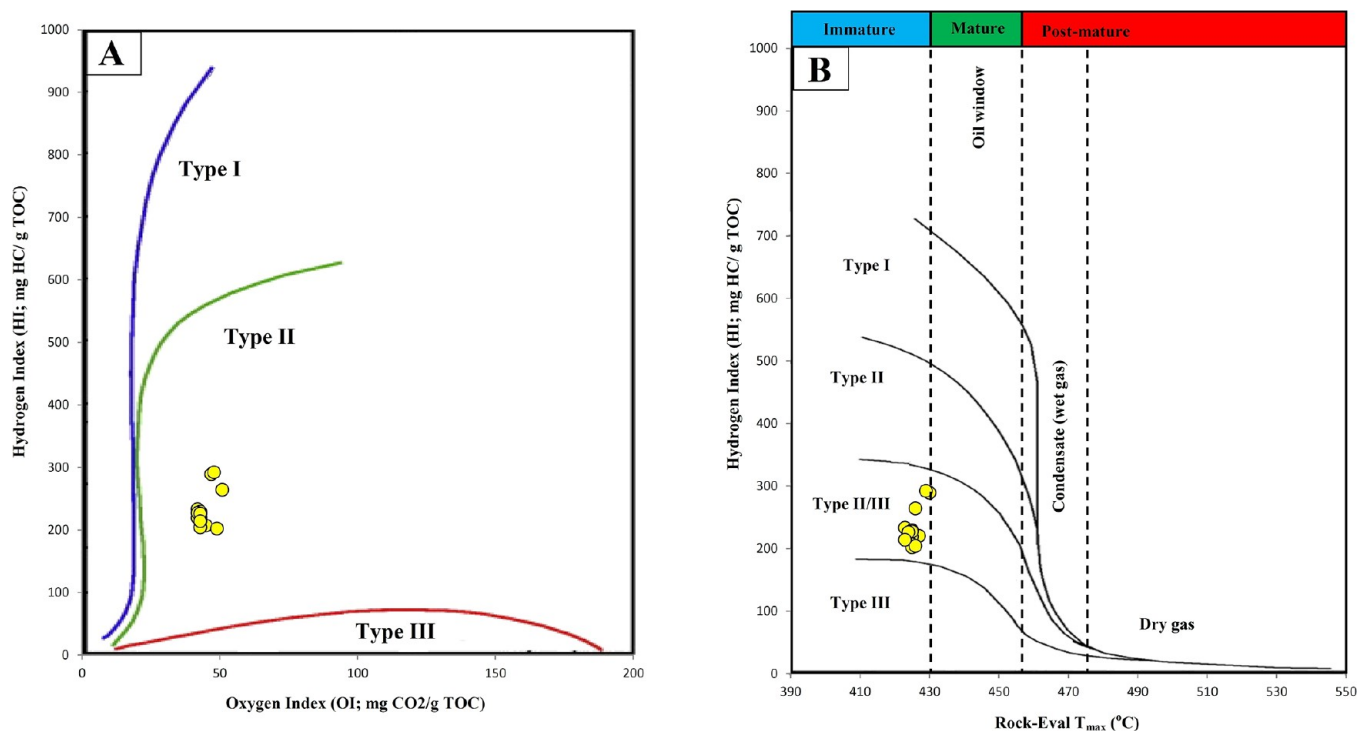
**Figure 10.** Geochemical correlations between the Rock-Eval hydrogen index (HI) with (A) oxygen index (OI) (B) and $T_{max}$, showing that the analyzed carbonaceous shale samples are dominated by type II/III kerogen at immature to early mature zones.

wt % implies a marine environment,[17] while a low S content of less than 0.5 wt % suggests a non-marine environment (freshwater).[16,18] Accordingly, the Kapurdi carbonaceous shales were generally deposited in a non-marine environment (i.e., lacustrine). This interpretation is further demonstrated by the relationship between TOC and sulfur contents (Figure 8).

**3.3. Rock-Eval Programmed Pyrolysis.** Table 2 also summarizes the $S_1$, $S_2$, $S_3$, HI, OI, and PI obtained by Rock-Eval pyrolysis of the 13 carbonaceous shale samples. According to the programmed pyrolysis results, the petroleum yields obtained by thermal cracking of kerogen ($S_2$) are substantial, ranging from 20.90 to 49.12 mg hydrocarbon/g rock (Table 2). Most of the samples tested ($n = 10$) had $S_2$ values greater than 30 mg hydrocarbon/g rock (range: 32.08−49.12 mg hydrocarbon/g rock), while three samples had the $S_2$ yields ranging from 20.90 to 27.65 mg hydrocarbon/g rock (Table 2). The pyrolysis data, on other hand, revealed that the examined samples have low free hydrocarbon yields ($S_1$), ranging from 0.28 to 0.68 mg hydrocarbon/g rock (Table 2). In this case, programmed pyrolysis $S_1$ and $S_2$ hydrocarbon yields in terms of petroleum yield (PY) were combined with TOC data for the analyzed samples and showed that the analyzed Kapurdi carbonaceous shales indicated organic matter richness and the capability of generating hydrocarbons, ranging from very good to excellent generating potential (Figure 9).

The $T_{max}$, based on the $S_2$ measurement, values were likewise measured during the pyrolysis analysis (Table 1). In this case, a maximum temperature ($T_{max}$) of $S_2$ generation was attained during the programmed pyrolysis analysis because the $S_2$ values surpass 1 mg/g rock.[19] In this respect, the $S_2$ values for most of the analyzed shale samples were found to be less than 1 (32.08− 49.12 mg HC/g rock) as shown in Table 2. Therefore, the Rock-Eval $T_{max}$ data was attained and was reliable, with values between 423 and 430 °C (Table 2). In this case, the analyzed Kapurdi

Member samples lie within the immature zone and they have yet to reach the optimum thermal maturity recovered for the generation of commercially viable volume of oil and gas.

In addition, the HI and OI values of the samples under consideration were calculated utilizing the compatibility of pyrolysis $S_2$ and $S_3$ yield with TOC content, respectively (Table 2). Therefore, the HI values of the analyzed samples vary from 207 to 292 mg hydrocarbon/g TOC (Table 2). Most of the analyzed samples ($n = 8$) have HI values of more than 220 mg HC/g TOC, with values ranging from 220 to 292 mg HC/g TOC (Table 2). The other five samples had the lowest HI values between 207 and 214 mg HC/g TOC (Table 2). In terms of OI values, 10 samples had values of <50 mg $CO_2$/g TOC, with the remaining sample having the highest value of 51 mg $CO_2$/g TOC (Table 2).

Traditionally, the HI and OI Rock-Eval data were used to classify the qualitative kerogen using modified van Krevelen diagrams.[14,18,20] The Rock-Eval pyrolysis results (i.e., the HI and OI) for the studied samples are comparable to kerogen types and indicate that most of the examined samples had mixed type II/ III (Figure 10A). In Figure 10B, this is illustrated on the modified van Krevelen diagram (HI vs $T_{max}$), revealing that the bulk of the examined shale samples are largely mixed type II/III (Figure 10B). As a result of these kerogen types, the analyzed carbonaceous shales in the Kapurdi Member of the Early Eocene Dharvi/Dunger Formation are expected to generate both oil and gas, with mainly oil generation potential (Figure 11).

**3.4. Open Pyrolysis-Gas Chromatography (Py-GC).** The Py-GC method provides critical insights about the composition of kerogens.[21,22] Additionally, the potential of petroleum generation and oil quality can also be predicted from GC analysis of pyrolysate $S_2$ materials.[21−24]

Figure 12 presents the Py-GC chromatograms of the extracted shale samples. The chromatograms indicate higher abundance
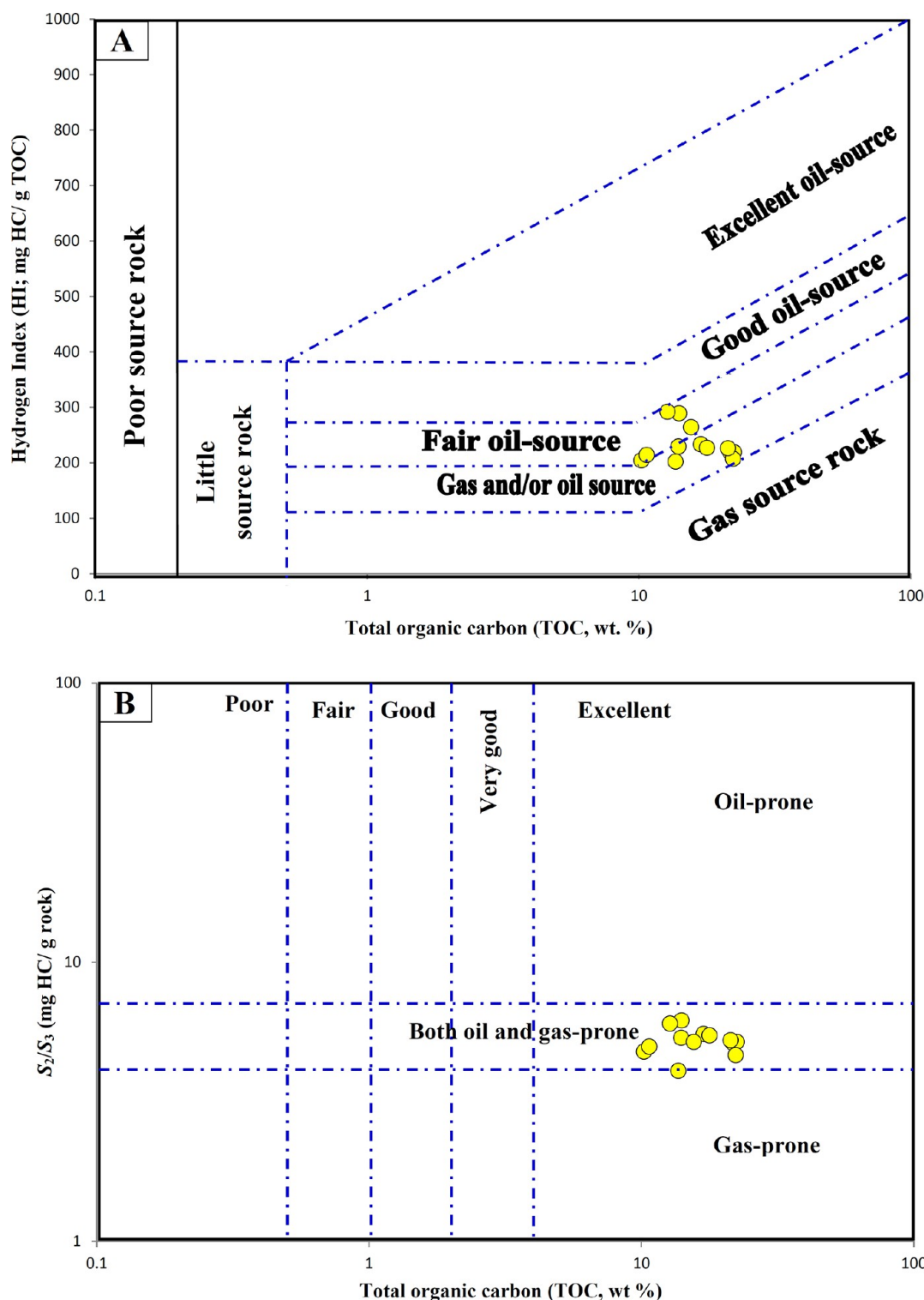
**Figure 11.** Geochemical correlation between TOC content and Rock-Eval data (A) HI and (B) ($S_2/S_3$), implying that the analyzed carbonaceous shale samples are both oil- and gas-prone source rocks, with high oil generation potential.

of the aliphatic compounds (*n*-alkene, *n*-alkane) along with relatively lower aromatic content. The distributions of the *n*-alkene and *n*-alkane are bimodal, with carbon numbers spanning from $C_5$ to beyond $C_{30}$. The bulk of the samples had substantial concentrations of *n*-alkene and *n*-alkane molecules in the low and high molecular carbon fractions. Toluene, xylene, and benzene alkylbenzenes are the most common aromatic hydrocarbon compounds. In addition to the aliphatic and aromatic

hydrocarbons, the pyrolysates include a significant amount of sulfur-derived organic compounds (Figure 12).

Based on the particular pyrolysate distributions of *n*-octane ($C_8$) and xylene (xy), several ratios were generated to decipher the kerogen types and their hydrocarbon generation potential.[23,25−27]

For example, oil-sourcing intervals exhibit $C_8$/xy ratio > 1 and it is less than 1 in the gas-prone sources. The kerogen type, on
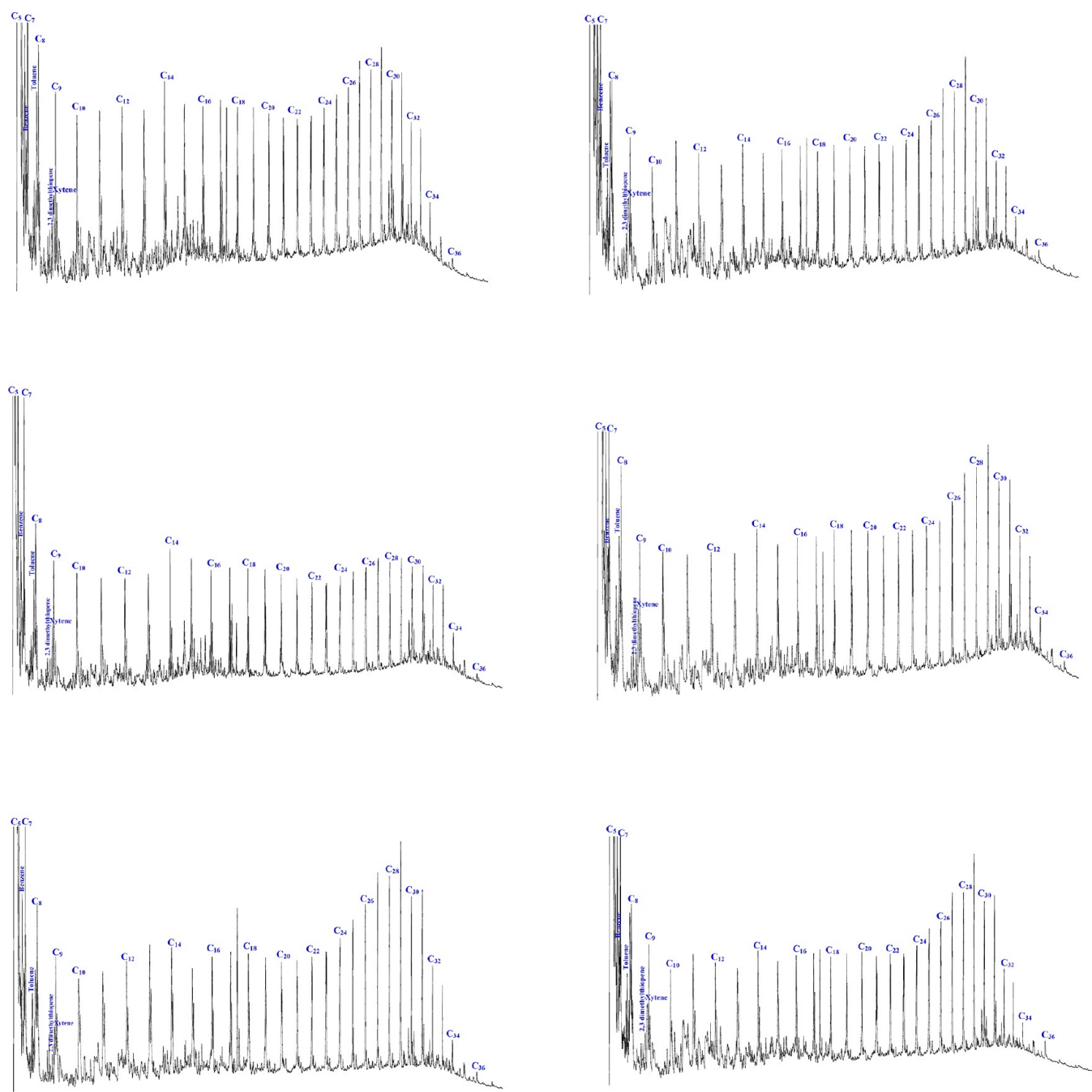
**Figure 12.** Pyrolysis GC pyrograms of the three analyzed carbonaceous shale samples, showing labeled peaks of *n*-alkene and *n*-alkane doublets, sulfur-lean organic matter, and aromatic hydrocarbons (toluene, xylene, and benzene) used as kerogen and petroleum-type proxies (see Figure 13).

the other hand, is defined by the proportion of xylene to *n*-octane given by the xy/$C_8$ index.[23] This index is divided into three categories, depending on their values. The type I and type II kerogens exhibit xy/$C_8$ usually lower than 0.4, while in combined II/III kerogens, it ranges from 0.4 to 1.3. In the type III kerogens, xy/C8 has been found to be greater than 1.3.[23]

The examined shale samples yield xy/$C_8$ values higher than 0.4 (0.50 to 1.17; see Table 2), indicating the dominance of mixed type II/III kerogens. Most of the samples investigated also had a $C_8$/xy ratio of 0.86 to 1.99 (Table 2), suggesting that these carbonaceous shales can generate a substantial volume of oil and gas at appropriate maturity ranges.[23,28,29]

In addition, the relative percentages of three pyrolysate compounds, namely, 2,3-dimethyldiophene, *ortho*-xylene, and carbon 9 (Table 2), were mapped on the ternary diagram of Eglinton et al.[30] The comparative proportions of pyrolysate compounds, i.e., total resolved $C_1$ to $C_5$ hydrocarbons, the total amount $C_6$ to $C_{14}$, and $C_{+15}$ of the *n*-alkenes/*n*-alkane ratios (Table 2), were utilized on the ternary diagram of Horsfield et al.[21] and notice that the dominating organic matter is largely type II/III kerogen (Figure 13A) and is expected to generate primarily paraffinic oils with high wax concentration may be produced (Figure 13B). The high potential waxy oil generation from these shales is confirmed by the presence of the significant fraction of the hydrogen-rich liptinite macerals such as sporinite,
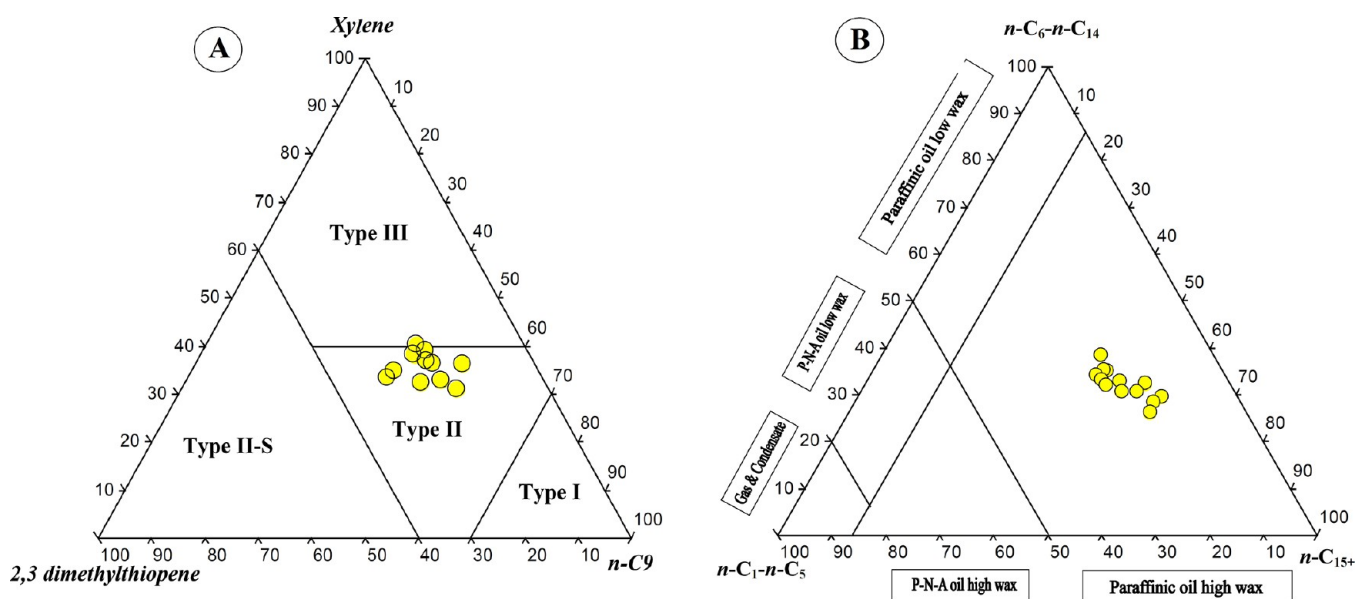
**Figure 13.** Ternary diagrams on (A) the kerogen characteristics based on the relative percentage of compounds 2,3-dimethylthiophene, O-xylene (1,2-dimethylbenzene), and n-non-l-ene (n-C9:1) and (B) the relative percentages of pyrolizate compounds, i.e., total resolved $C_1$ to $C_5$ hydrocarbons, the sum $C_6$ to $C_{14}$, and $C_{+15}$ of the n-alkenes/n-alkane ranges that derived from the n-alkyl chain length distribution in the Py-GC data (see Figure 7), showing that the analyzed carbonaceous shale samples are dominated by type II/III kerogen and can generate mainly high waxy oil.
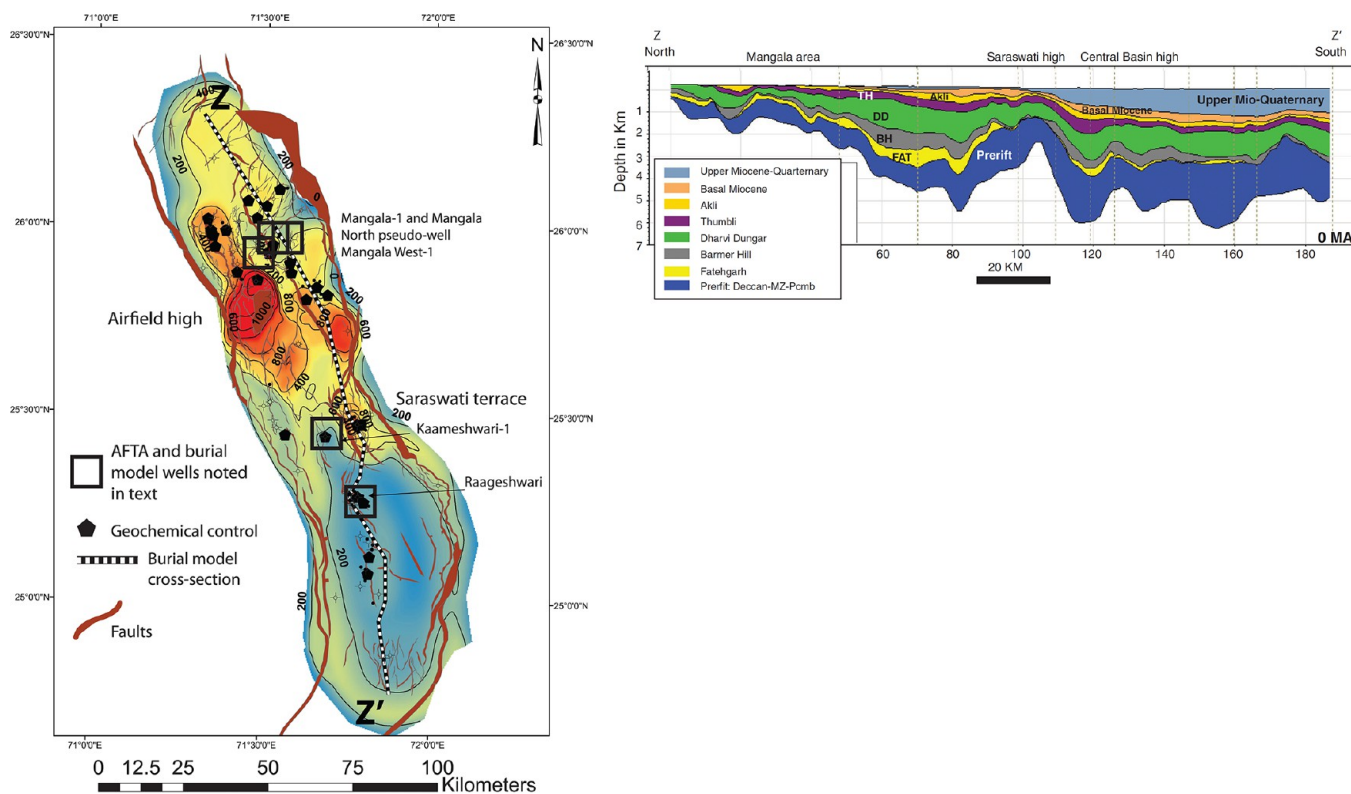


**Figure 14.** Right: map of geochemical control and total erosion map for the Barmer Basin, showing the thickness of sediments eroded in meters and the location of wells used for vitrinite, spore coloration. Left: north−south cross section through the present day and restored pseudo-basin model. Note that the northern basin has not been buried as deeply as the central and southern part of the basin.[1]

resinite, cutinite, and suberinite in the analyzed samples (Figure 6).

**3.5. Implications for Further Petroleum Exploration Opportunities.** The current technological advancements have enhanced society's dependence on fuel and have triggered hydrocarbon exploration activities around the globe. Con-

sequently, the search for source rocks is on the rise and can be used to establish new frontiers. It is essential to understand the source rock properties and their distribution within various depositional sequences. That is why petroleum geoscience has emerged as a vital research theme.[31−34]

The hydrocarbon generation phases are controlled by specific parameters such as temperature and pressure.[35] Scientists repeatedly design studies to establish conditions that are representative of geological settings of the petroleum generation process. However, a complete understanding of the petroleum generation process involves the integration of a sedimentary basin's source rock, moderated by the variables influenced by tectonics, paleogeography, distribution and paleoenvironmental deposition, and is an essential step leading to a sophisticated development, exploration, and utilization of prevailing hydrocarbon reserves.[36,37]

This section discusses the geochemical and petrological properties of the Kapurdi carbonaceous shale within the early Eocene Dharvi/Dunger Formation and their distribution in the Barmer Basin using the integration of the geochemical results of this study and previous works,[1] thus contributing to successful exploration attempts.

Organic matter intervals in the shales within the Late Paleocene Barmer Hill Formation and the Early Eocene Dharvi/Dunger Formation have dominated petroleum development in the Barmer Basin, with proven oil- and gas-prone source rocks.[1] The Barmer Hill Formation is believed to be the main oil source rock, being more mature than the Dharvi/Dunger Formation.[1,3] This discovery provides substantial geochemical links between oil-source rocks and reveals that most of the discovered oils in the basin were derived from organic matter in the Barmer Hill source rock.[3] Thus, the Late Paleocene Barmer Hill Formation is a promising candidate as a conventional petroleum source rock, fueling exploration operations throughout the basin in search of petroleum resources.

The results of this study reveal that the carbonaceous shale intervals of the Early Eocene Dharvi/Dunger Formation are potential source rocks for predominantly oil- and limited gas-prone. They display relatively low maturity (immature to early mature oil-window), implying that commercial quantities of oil have yet to be generated.

However, because of tectonics, paleogeography, and paleoenvironmental deposition, the Dharvi/Dunger Formation is equivalent throughout the Barmer Basin in many ways.[1] According to Dolson et al.,[1] the primary difference between the Dharvi/Dunger Formations across the Barmer Basin (including this research) is connected to burial depths. This indicates that the Dharvi/Dunger source rock in different portions of the basin likely achieved substantially different levels of thermal maturity because of burial temperatures and so may have produced commercial HCs gas in the basin's deeper regions.

According to Dolson et al.,[1] as one goes north through the Barmer Basin's central and southern parts, the burial depths of the Dharvi/Dunger Formation increase (Figure 14). As a result, the Barmer Basin's central and southern regions have a greater potential for hydrocarbon extraction than the northern half. This vital discovery will be advantageous for potential prospect and exploration targets in the Barmer Basin, where proven deeper source rock positions make them viable candidates for conventional petroleum resources. This conclusion is also supported by high abundance of petroleum discoveries in the Barmer Basin's central and southern regions.[1]

The Dharvi/Dunger Formation reached a burial depth of more than 3000 m in the basin's central and southern parts, as seen in Figure 16. The high organic composition (maximum TOC = 22.42 wt %) in the Dharvi/Dunger shales together with their geological location at more than 3 km deep makes them ideal source rocks for commercial oil or/and gas HCs. As a result, in conjunction with the previous work of Dolson et al.,[1] the significant abundance of oil generation potential associated with the Early Eocene Dharvi/Dunger Formation, as highlighted in this study, may serve as a critical reference for future conventional petroleum exploration in the Barmer Basin, where these organic-rich shale units may have reached a peak mature oil generation window. As a result, the idea that future petroleum exploration and production should focus on northwest India's Barmer Basin gains substantial scientific credence.

## 4. CONCLUSIONS

This work has reported the characteristics of organic matter input into the Kapurdi carbonaceous shale of the Early Eocene Dharvi/Dunger Formation in the onshore Barmer Basin, Northwestern India performed using comprehensive geochemical and petrological investigations. From this study, the key takeaways have been drawn as follows

1- The analyzed Kapurdi carbonaceous shales have high TOC content in the range between 10.24% and 22.43% and petroleum potential of up to 49.63 mg hydrocarbon/g rock, making them expected to be favorable source rocks for petroleum generation.

2- In terms of organic facies (kerogen type), most of the analyzed Kapurdi carbonaceous shales contain a mixture of organic matter of types II and III kerogen, with HI values between 202 HC/g TOC and 292 HC/g TOC. This indicates their probability as oil/gas source rocks, with high oil generation potential.

3- The dominant aliphatic $n$-alkenes/$n$-alkanes, with significant amounts of aromatic components, shown in the Py-GC results, are in good agreement with the bulk pyrolysis HI values. They confirm that the studied Kapurdi carbonaceous shale rocks contain primarily mixed type II and III kerogens.

4- Kerogen types of mixed II and III and their contributions to hydrocarbon (oil and gas) generation potential were also confirmed by the high proportion of huminite and liptinitic macerals.

5- Most of the studied carbonaceous shale rocks are currently at a lower maturity level, ranking from immature to very early mature of oil generation window as demonstrated by low maturity values (i.e., $T_{max}$ up to 430 °C and VR$_o$ up to 0.52). Therefore, the organic matter in the studied rocks has not yet been altered sufficiently to generate commercial oil/gas volumes.

6- This study can be a foundation for further petroleum exploration in the Barmer Basin in NW India, especially in the central and southern sections of the basin. Where these carbonaceous shale rocks of the Dharavi/Dungar Formation have relatively deep stratigraphic sections, and high maturity levels are anticipated for petroleum exploration and production.

## ■ AUTHOR INFORMATION

### Corresponding Author

**Mohammed Hail Hakimi** — *Geology Departments, Faculty of Applied Science, Taiz University, 6803 Taiz, Yemen; Department of Petroleum Engineering, Kazan Federal University, Kazan 420008, Russia;* ◉ orcid.org/0000-0002-3320-9690; Email: ibnalhakimi@yahoo.com

## Authors

**Alok Kumar** — *Department of Geology, University of Malaya, 50603 Kuala Lumpur, Malaysia*

**Alok K. Singh** — *Petroleum Engineering and Geoengineering, Rajiv Gandhi Institute of Petroleum Technology, Jais, Amethi 229 304, India*

**Wan Hasiah Abdullah** — *Department of Geology, University of Malaya, 50603 Kuala Lumpur, Malaysia*

**Nor Syazwani Zainal Abidin** — *Geosciences Department, Faculty of Science and Information Technology, Universiti Teknologi PETRONAS, 32610 Bandar Seri Iskandar, Perak, Malaysia*

**Afikah Rahim** — *School of Civil Engineering, Faculty of Engineering Universiti Teknologi Malaysia, Skudai, Johor 81310, Malaysia*

**Khairul Azlan Mustapha** — *Department of Geology, University of Malaya, 50603 Kuala Lumpur, Malaysia*

**Nura Abdulmumini Yelwa** — *Department of Geology, University of Malaya, 50603 Kuala Lumpur, Malaysia; Department of Geology, Usmanu Danfodiyo University, Sokoto 840004, Nigeria;* ● orcid.org/0000-0002-7454-2326

Complete contact information is available at:
https://pubs.acs.org/10.1021/acsomega.2c05148

## Notes

The authors declare no competing financial interest.

## ■ REFERENCES

(1) Dolson, J.; Burley, S. D.; Sunder, V. R.; Kothari, V.; Naidu, B.; Whiteley, N. P.; Farrimond, P.; Taylor, A.; Direen, N.; Ananthakrishnan, B. The discovery of the Barmer Basin, Rajasthan, India, and its petroleum geology. *AAPG Bull.* **2015**, *99*, 433−465.

(2) Zhu, B.; Kidd, W. S.; Rowley, D. B.; Currie, B. S.; Shafique, N. Age of initiation of the India-Asia collision in the east-central Himalaya. *J. Geol.* **2005**, *113*, 265−285.

(3) Farrimond, P.; Naidu, B. S.; Burley, S. D.; Dolson, J.; Whiteley, N.; Kothari, V. Geochemical characterization of oils and their source rocks in the Barmer Basin, Rajasthan, India. *Pet. Geosci.* **2015**, *21*, 301−321.

(4) Taylor, G. H.; Teichmüller, M.; Davis, A. C. F. K.; Diessel, C. F. K.; Littke, R.; Robert, P. *Organic petrology*, 1998.

(5) Hower, J. C.; Wagner, N. J. Notes on the methods of the combined maceral/micro-lithotype determination in coal. *Int. J. Coal Geol.* **2012**, *95*, 47−53.

(6) Pickel, W.; Kus, J.; Flores, D.; Kalaitzidis, S.; Christanis, K.; Cardott, B. J.; Misz-Kennan, M.; Rodrigues, S.; Hentschel, A.; Hamor-Vido, M.; Crosdale, P.; Wagner, N. Classification of liptinite (ICCP System 1994). *Int. J. Coal Geol.* **2017**, *169*, 40−61.

(7) ICCP. The new inertinite classification (ICCP System 1994). *Fuel* **2001**, *80*, 459−471.

(8) Lafargue, E.; Marquis, F.; Pillot, D. Rock-Eval 6 applications in hydrocarbon exploration, production, and soil contamination studies. *Rev. Inst. Fr. Pet.* **1998**, *53*, 421−437.

(9) Peters, K.; Cassa, M. Applied source rock geochemistry. In Magoon, LB; WG, Dow ed, *The petroleum system from source to trap. AAPG memoir.* 1994, *60*, 93−117.

(10) Larter, S. R. Application of analytical pyrolysis techniques to kerogen characterization and fossil fuel exploration/exploitation, In K., Voorhees (Ed.), *Analytical Pyrolysis*. Butterworths, London: Heinemann, 1984, pp. 212−275.

(11) Petersen, H. I.; Øverland, J. A.; Solbakk, T.; Bojesen-Koefoed, J. A.; Bjerager, M. Unusual resinite-rich coals found in northeastern Greenland and along the Norwegian coast: Petrographic and geochemical composition. *Int. J. Coal Geol.* **2013**, *109−110*, 58−76.

(12) Abdullah, W. H.; Togunwa, O. S.; Makeen, Y. M.; Hakimi, M. H.; Mustapha, K. A.; Baharuddin, M. H.; Sia, S. G.; Tongkul, F. Hydrocarbon source potential of Eocene−Miocene sequence of western Sabah, Malaysia. *Mar. Pet. Geol.* **2017**, *83*, 345−361.

(13) Hakimi, M. H.; Ahmed, A.; Kahal, A. Y.; Salad Hersi, O.; Al Faifi, H. J.; Qaysi, S. Organic geochemistry and basin modeling of Late Cretaceous Harshiyat Formation in the onshore and offshore basins in Yemen: Implications for effective source rock potential and hydrocarbon generation. *Mar. Pet. Geol.* **2020**, *122*, 10470.

(14) Makeen, Y. M.; Abdullah, W. H.; Abdul Ghofur, M. N.; Ayinla, H. A.; Hakimi, M. H.; Shan, X.; Mustapha, K. A.; Kamal Shuib, M.; Liang, Y.; Zainal Abidin, N. S. Hydrocarbon generation potential of Oligocene oil shale deposit at onshore Penyu Basin, Chenor, Pahang, Malaysia. *Energy Fuels* **2019**, *33*, 89−105.

(15) Katz, B.; Lin, F. Lacustrine basin unconventional resource plays: Key differences. *Mar. Pet. Geol.* **2014**, *56*, 255−265.

(16) Berner, R. A.; Raiswell, R. Burial of organic carbon and pyrite sulfur in sediments over Phanerozoic time: a new theory. *Geochim. Cosmochim. Acta* **1983**, *47*, 855−862.

(17) Hakimi, M. H.; Abdullah, W. H.; Alqudah, M.; Makeen, Y. M.; Mustapha, K. A. Reducing marine and warm climate conditions during the Late Cretaceous, and their influence on organic matter enrichment in the oil shale deposits of North Jordan. *Int. J. Coal Geol.* **2016**, *165*, 173−189.

(18) Makeen, Y. M.; Abdullah, W. H.; Hakimi, M. H.; Mustapha, K. A. Source rock characteristics of the Lower Cretaceous Abu Gabra Formation in the Muglad Basin, Sudan, and its relevance to oil generation studies. *Mar. Pet. Geol.* **2015**, *59*, 505−516.

(19) Katz, B.; Lin, F. Consideration of limitations of thermal maturity with respect to vitrinite reflectance, $T_{max}$ and other proxies. *AAPG* **2021**, *105*, 695−720.

(20) Mukhopadhyay, P. K.; Wade, J. A.; Kruge, M. A. Organic facies and maturation of Jurassic/Cretaceous rocks, and possible oil-source rock correlation based on pyrolysis of asphaltenes, Scotion Basin. Canada. *Org. Geochem.* **1995**, *22*, 85−104.

(21) Horsfield, B. Practical criteria for classifying kerogens: Some observations from pyrolysis−gas chromatography. *Geochim. Cosmochim. Acta* **1989**, *53*, 891−901.

(22) Dembicki, H., Jr. Improved determination of source quality and kerogen type by combining rock eval and pyrolysis-gas chromatography results (abs.). *AAPG Annual Convention Program* **1993**, *2*, 90.

(23) Dembicki, H., Jr. Three common source rock evaluation errors made by geologists during prospect or play appraisals. *AAPG Bull.* **2009**, *93*, 341−356.

(24) Abbassi, S.; Edwards, D. S.; George, S. C.; Volk, H.; Mahlstedt, N.; di Primio, R.; Horsfield, B. Petroleum potential and kinetic models for hydrocarbon generation from the Upper Cretaceous to Paleogene Latrobe group coals and shales in the Gippsland Basin Australia. *Org. Geochem.* **2016**, *91*, 54−67.

(25) Hasiah, A. W. Oil-generating potential of tertiary coals and other organic-rich sediments of the Nyalau Formation, onshore Sarawak. *J. Asian Earth Sci.* **1999**, *17*, 255−267.

(26) Mustapha, K. A.; Abdullah, W. H. Petroleum source rock evaluation of the Sebahat and Ganduman Formations, Dent Peninsula, Eastern Sabah Malaysia. *J. Asian Earth Sci.* **2013**, *76*, 346−355.

(27) Adegoke, A. K.; Abdullah, W. H.; Hakimi, M. H. Geochemical and petrographic characterisation of organic matter from the Upper Cretaceous Fika shale succession in the Chad (Bornu) Basin, northeastern Nigeria: Origin and hydrocarbon generation potential. *Mar. Pet. Geol.* **2015**, *61*, 95−110.

(28) Hakimi, M. H.; Abdullah, W. H.; Sia, S. G.; Makeen, Y. M. Organic geochemical and petrographic characteristics of tertiary coals in the northwest Sarawak, Malaysia: Implications for palaeoenvironmental conditions and hydrocarbon generation potential. *Mar. Pet. Geol.* **2013**, *48*, 31−46.

(29) Hakimi, M. H.; Abdullah, W. H.; Mustapha, K. A.; Adegoke, A. K. Petroleum generation modeling of the Late Cretaceous coals from the Jiza-Qamar Basin as infer by kerogen pyrolysis and bulk kinetics. *Fuel* **2015**, *154*, 24−34.

(30) Eglinton, T. I.; Sinninghe Damsté, J. S.; Kohnen, M. E. L.; de Leeuw, J. W. Rapid estimation of the organic sulphur sulfur content of kerogens, coals and asphaltenes by pyrolysis-gas chromatography. *Fuel* **1990**, *69*, 1394−1404.

(31) Chapman, R. E. *Petroleum geology*. Elsevier: Netherlands 2000.

(32) Loucks, R. G.; Reed, R. M.; Ruppel, S. C.; Jarvie, D. M. Morphology, genesis, and distribution of nanometer−scale pores in siliceous mudstones of the Mississippian Barnett shale. *J. Sediment. Res.* **2009**, *79*, 848−861.

(33) Wu, J.; Liang, C.; Hu, Z. Q.; Yang, R. C.; Xie, J.; Wang, R. Y.; Zhao, J. H. Sedimentation mechanisms and enrichment of organic matter in the Ordovician Wufeng Formation-Silurian Longmaxi Formation in the Sichuan Basin. *Mar. Pet. Geol.* **2019**, *101*, 556−565.

(34) Qadri, S. M. T.; Islam, M. A.; Shalaby, M. R.; El-Aal, A. K. A. Reservoir quality evaluation of the Farewell sandstone by integrating sedimentological and well log analysis in the Kupe South Field, Taranki Basin-New Zealand. *J. Pet. Explor. Prod. Technol.* **2021**, *11*, 11−31.

(35) Ungerer, P.; Burrus, J.; Doligez, B. P. Y. C.; Chenet, P. Y.; Bessis, F. Basin evaluation by integrated two-dimensional modeling of heat transfer, fuid fow, hydrocarbon generation, and migration. *AAPG Bull.* **1990**, *74*, 309−335.

(36) Magoon, L. B.; Valin, Z. C. Overview of petroleum system case studies. *AAPG Mem.* **1994**, *60*, 329−338.

(37) Qadri, S. M.; Islam, M. A.; Shalaby, M. R.; Ali, S. H. Integration of 1D and 3D modeling schemes to establish the farewell formation as a self-sourced reservoir in Kupe field, Taranaki basin New Zealand. *Front. Earth Sci.* **2020**, 1.